Carbohydrate Polymers 97 (2013) 152–158

Contents lists available at SciVerse ScienceDirect

Carbohydrate Polymers

journal homepage: www.elsevier.com/locate/carbpol

Chitosan fibers enhanced gellan gum hydrogels with superior mechanical properties and water-holding capacity

Limei Liu [a], Binghao Wang [b], Yuan Gao [a], Tong-chun Bai [a,*]

[a] Institute of Physical Chemistry, College of Chemistry, Chemical Engineering and Materials Science, Soochow University, Suzhou, Jiangsu 215123, China
[b] Jiangsu Key Laboratory of Advanced Functional Polymer Design and Application, Department of Polymer Science and Engineering, College of Chemistry, Chemical Engineering and Materials Science, Soochow University, Suzhou, Jiangsu 215123, China

ARTICLE INFO

Article history:
Received 17 October 2012
Received in revised form 25 February 2013
Accepted 12 April 2013
Available online 24 April 2013

Keywords:
Chitosan fibers
Gellan gum
Dehydration
Mechanical property
Water-holding capacity

ABSTRACT

New hydrogels based on acetylated gellan gum (A-gellan) and chitosan fibers (F-chitosan) are prepared and coded as F-chitosan/A-gellan. Compared to A-gellan hydrogel, F-chitosan/A-gellan hydrogels show higher storage moduli and water-holding capacity. Specifically, the storage modulus of 2.0 F-chitosan/A-gellan (mass ratio of chitosan fibers and gellan gum is 2:1) hydrogels at regular frequency of 1 rad/s is 2.2 kPa, approximately 4.6 times more than that of the A-gellan hydrogel. In addition, the fractural morphology analysis of A-gellan and 2.0 F-chitosan/A-gellan hydrogels treated by different dry methods indicates that the 2.0 F-chitosan/A-gellan hydrogel has more stable macrostructure. Moreover, compared to A-gellan gel, 2.0 F-chitosan/A-gellan gel shows higher activation energy and water-holding capacity during dehydration and higher dielectric constant after dehydration. These results can be attributed to the special advantages of chitosan fibers, which are full of polar and hydrophilic amino group and can transfer the load applied on the hydrogels in fiber form.

1. Introduction

Hydrogels are promising candidates for the development of engineered tissues, either as scaffolds for supporting cell growth or as cell carrier and delivery systems, mainly due to their structural similarity to the extracellular matrix (ECM) of tissues (Coutinho et al., 2012), such as the highly hydrated three-dimensional structure and diffusive transport property. In recent years, research interests have shifted from synthetic materials to polysaccharide hydrogels as they show better biocompatibility and controllable properties and are abundant in resource (Swetha et al., 2010; Vlierberghe, Dubruel, & Schacht, 2011). However, the great challenge for polysaccharide hydrogels in tissue engineering applications, especially those requiring extensive load-bearing behavior, is their low mechanical property (Muzzarelli, Greco, Busilacchi, Sollazzo, & Gigante, 2012). Therefore, developing polysaccharide hydrogels with high mechanical strength is a priority for expanding the range of applications of hydrogels.

Among polysaccharide hydrogels, gellan gum, a natural polysaccharide and FDA-approved food additive, has been introduced for tissue engineering application in recent years (Oliveira et al., 2010; Smith, Shelton, Perrie, & Harris, 2007). Fan's group synthesized a complex hydrogel based on modified gellan gum and carboxymethyl chitosan. The double-network hydrogel significantly decreased the gelation temperature of gellan gum to below physiological temperature and increased its compression modulus to 278 kPa (Tang, Sun, Fan, & Zhang, 2012). Dong-An Wang's group prepared synovium-derived mesenchymal stem cells (SMSC) laden gellan hydrogels to investigate the viability of SMSC in hydrogels treated with TGF-β1, TGF-β3 and BMP-2, which laid a foundation for their potential application in clinical cartilage repair (Fan et al., 2010). Ali Khademhosseini's group reported a double-network photocrosslinkable gelatin and gellan gum hydrogel, which enhanced the mechanical properties and cell-encapsulated ability of polysaccharide hydrogel (Shin, Olsen, & Khademhosseini, 2012).

These researches have pictured the great importance and feasible application of gellan gum hydrogel. However, like other polysaccharides, the hydrogel formed by gellan gum shows poor mechanical strength, which hinders its further use. To the best of our knowledge, fiber-containing gellan gum hydrogels are feasible materials and their mechanical behavior hasn't been reported in other works. Also, the structural characterization of gellan gum hydrogels hasn't been discussed in detail previously. Therefore, it is of great interest to develop new gellan gum composite hydrogel with high mechanical performance, and then to discuss the relationship between structures and properties.

Chitosan, composed of glucosamine and *N*-acetyl glucosamine monomers, is well known as a biocompatible, biodegradable, nontoxic material. In particular, its chemical structure is analogous

* Corresponding author. Tel.: +86 512 65880363; fax: +86 512 65880089.
E-mail address: tcbai@suda.edu.cn (T.-c. Bai).

0144-8617/$ – see front matter © 2013 Elsevier Ltd. All rights reserved.
http://dx.doi.org/10.1016/j.carbpol.2013.04.043

with various glycosaminoglycans (GAGs) and hyaluronic acid found in articular cartilage, making it an ideal scaffolding material in articular cartilage engineering (Muzzarelli, 2009; Suh & Matthew, 2000). Chitosan fibers, made of chitosan, can play a role in transferring load with fiber form. They have both the advantages of chitosan and fibers, and have been widely used to produce surgical suture, surgical dressings, and health underwear (Tuzlakoglu, Alves, Mano, & Reis, 2004).

In this paper, chitosan fibers were first introduced into gellan gum hydrogels. Due to the advantage of fibriform chitosan, a great improvement in mechanical strength has been achieved. In addition, the swelling and dehydration process of the hydrogels were systematically studied. Some unexpected but interesting phenomena were discovered and discussed.

2. Experimental

2.1. Materials

The chitosan fibers were purchased from Shandong Weifang Youngchito Bio. Co. Ltd. The raw material chitosan powder with a 90% degree of deacetylation and weight-average molecular weight of 4×10^5–5×10^5 was also produced by this company. The chitosan fibers we used here were prepared by utilizing wet spinning technique with a purity of 98% chitosan powder, the breaking strength of a single chitosan fiber with the average diameter of 10–20 μm and the lengths of 1 mm is 2.0 cN/dtex. The edible grade fully acetylated gellan gum with number average molecular weight of 1×10^6–2×10^6 was supplied by Jinan Deke Biotechnology Co. Ltd. Phosphate Buffered Saline (PBS) was provided by Beijing Solarbio Science & Technology Co. Ltd, the PH of the solution is 7.2–7.4.

2.2. Preparation of A-gellan hydrogel

1.6 wt % aqueous solution of A-gellan was prepared, and then the solution was placed in 85 °C water bath and stirred for another 5 min. After that, it was poured into a mold and cooled to room temperature. The resultant hydrogels are denoted as A-gellan.

2.3. Preparation of F-chitosan/A-gellan hydrogels

1.6 wt % aqueous solution of A-gellan was prepared, and then chitosan fibers were uniformly added with the mass ratios of between chitosan fibers and gellan gum are 1:2, 1:1 and 2:1, respectively. Then the solutions were placed in 85 °C water bath and stirred for another 5 min. After that, they were poured into a mold and cooled to room temperature. The resultant hydrogels are denoted as *n*F-chitosan/A-gellan, where *n* is the mass ratio of chitosan fibers and gellan gum.

2.4. Rheological analysis

Rheological characterization of hydrogel samples were performed on a Haake Rheostress 6000 rheometer (Thermo Electron Co., Karslruhe, Germany). The oscillation shear flow measurement was conducted at 37 °C, a shear stress of 1 Pa (plate–plate geometry) and the angular frequency range from 0.1 to 100 rad/s. A layer of oil was added to prevent evaporation, and the measuring gap size is 0.5 mm.

2.5. Morphology characterization

A scanning electron microscope (Hitachi S-4700, Tokyo, Japan) was employed to observe the morphologies of the hydrogels after freeze-drying and oven-drying.

2.6. Characterization of swelling behavior

The dried F-chitosan/A-gellan hydrogels (approximately 0.02 g) were immersed in PBS or in deionized water at 37 °C. The swollen weight was determined by weighting after wipe off the surface water. The swelling ratio (Q) was calculated from Eq. (1) (Brazel & Peppas, 1995).

$$Q = \frac{W_s - W_d}{W_d} \times 100\% \quad (1)$$

where W_d and W_s are the weight of the samples in the dry and swollen states, respectively.

When the hydrogels kept in solutions reached the equilibrium swelling, the aqueous solution content of the swollen gel (W) was calculated from Eq. (2) (Siegel & Firestone, 1988).

$$W = \frac{W_{es} - W_d}{W_{es}} \times 100\% \quad (2)$$

where W_{es} is the weight of the samples in the equilibrium swelling states.

2.7. Dehydration kinetic measurements

Differential scanning calorimetry (DSC) measurements were performed on a Netzsch DSC 204F1 apparatus (Selb, Germany). The samples were examined from 30 °C to 120 °C at different heating rates (β_i) of 1, 2, 3, 4 and 5 °C min^{-1} in a nitrogen atmosphere.

2.8. Dielectric properties measurements

Dielectric constant and dielectric loss tangent were measured using a broadband dielectric spectrometer (Novocontrol Concept 80, Hundsangen, Germany) at room temperature over a wide frequency range (from 1 to 10^7 Hz). The thickness of dried hydrogel was 0.1 mm.

3. Results and discussion

3.1. Rheological analysis

The mechanical properties of the hydrogels were examined by oscillatory rheological experiments as a function of frequency. Fig. 1 shows the changes in the storage moduli (G'), the loss moduli (G'') for the hydrogels. The G', reflecting the elasticity, which is defined as the stored energy due to the elastic deformation, and the G'' reflects the viscosity of hydrogels (Pelletier et al., 2001). The G' of all the hydrogels is independent on the frequency at first, and then gradually increases with the increasing frequency. This is attributed to the relationships between the chain segments and frequency. When the shear frequency is low, the A-gellan macromolecular chains can keep up with change of frequency, and the hysteresis effect is very low. As the frequency further increases, the chain segments are stretched, orientated, and deviated from the minimum energy balance point (Liu, Shao, Chen, & Zheng, 2006). Therefore, they can not keep up the movement of frequency and G' increase with the increasing frequency. Additionally, the inflection point of A-gellan and F-chitosan/A-gellan hydrogels increases with the increasing content of chitosan fibers indicates that elastic chitosan fibers can accommodate F-chitosan/A-gellan hydrogels to the higher movement frequency, which can be applied to intense conditions.

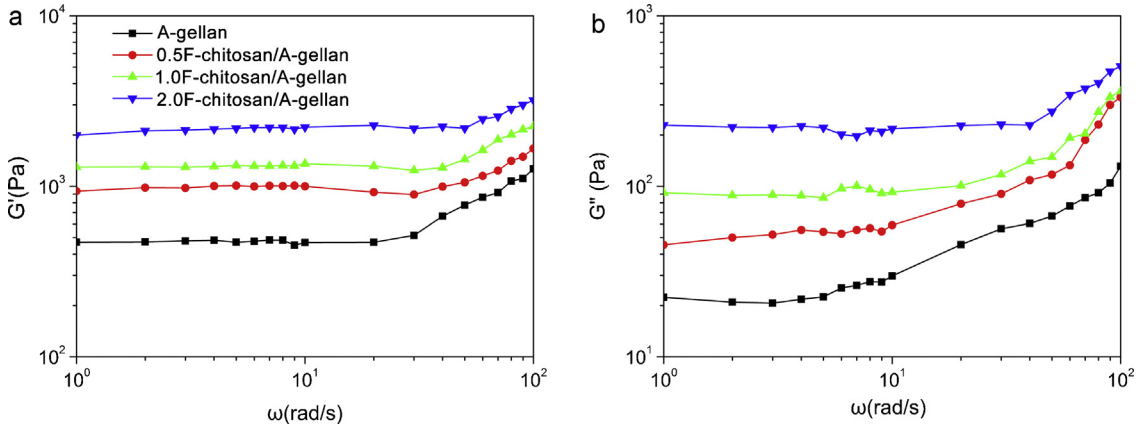

Fig. 1. Frequency dependence of storage moduli and loss moduli of the A-gellan and F-chitosan/A-gellan hydrogels.

Furthermore, when the content of chitosan fibers increases, both the G' and G'' values of F-chitosan/A-gellan hydrogels increase gradually. This is because when the hydrogels were subject to external forces, the matrix would transfer the load to the chitosan fibers, thus can enhance the strength of hydrogels (Silva et al., 2008). Specifically, the G' of the 2.0 F-chitosan/A-gellan hydrogel is 2.2 kPa at an angular frequency of 1 rad/s, which is 4.6 times more than that of A-gellan hydrogel.

3.2. Morphology

Compared to A-gellan hydrogel, the 2.0 F-chitosan/A-gellan hydrogel shows higher whole stability, this was characterized by SEM study. Fig. 2a and b are the fractured surface of A-gellan gel after freeze-drying and oven drying, respectively. Fig. 2c and d are the fractured surface of 2.0 F-chitosan/A-gellan gel after freeze-drying and oven drying, respectively. It is well known that the freeze-drying treatment has a far smaller damage to macrostructure of hydrogel than oven drying treatment (Zhu, Chan-Park, & Gao, 2006). We can see from the Fig. 2a and c, both the A-gellan gel and 2.0 F-chitosan/A-gellan gel contain pores with size of 10–20 μm. However, after oven drying treatment, the structure of the gel will ruin to a large extent. As can be seen from Fig. 2b, the fractured surface of A-gellan gel has formed a dense layer without any pores. In contrast, there are still a lot of pores in the 2.0 F-chitosan/A-gellan gel as shown in Fig. 2d. This is because chitosan fibers were interspersed between the holes, thereby reducing the collapse of the holes and maintaining the structural stability of the hydrogels. This is also confirmed by the fact that the 2.0 F-chitosan/A-gellan hydrogel shows a higher storage modulus than A-gellan hydrogel.

3.3. Swelling behavior of the hydrogels

The swelling degree of the hydrogels in PBS as a function of chitosan fibers content was characterized in Fig. 3a. The rate of water

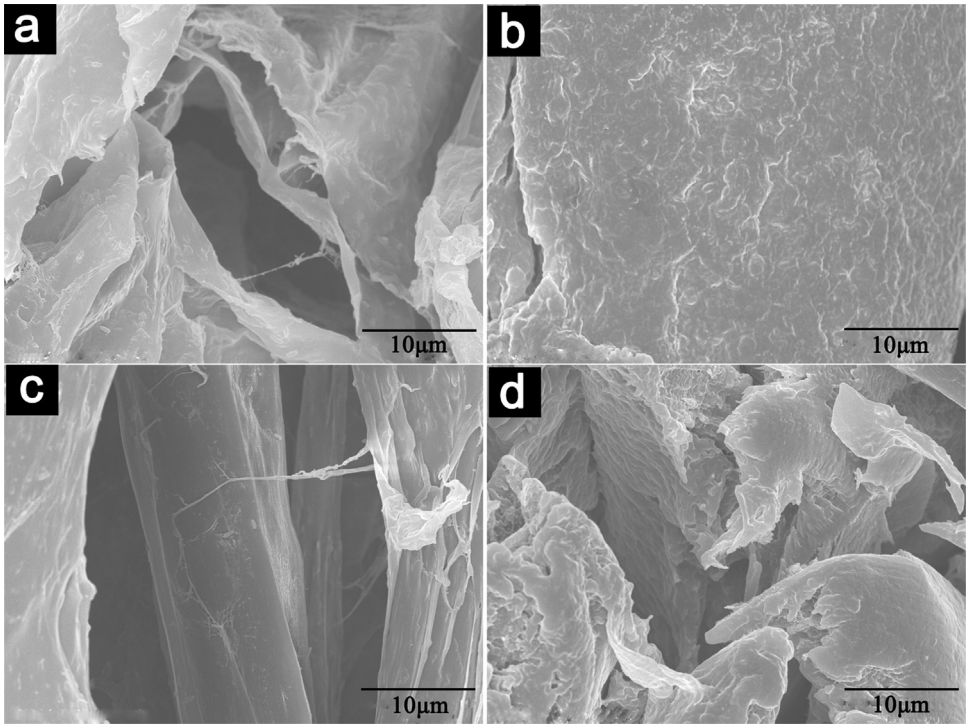

Fig. 2. The fractured surface of A-gellan gel after (a) freeze-drying and (b) oven drying. The fractured surface of 2.0 F-chitosan/A-gellan gel after (c) freeze-drying and (d) oven drying.

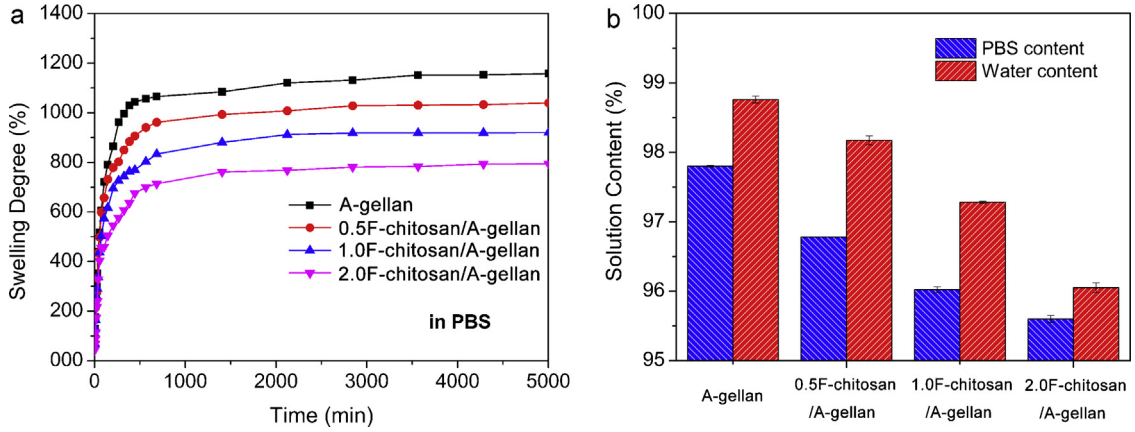

Fig. 3. (a) The swelling degree of A-gellan and F-chitosan/A-gellan hydrogels changes with time in PBS. (b) The equilibrium solvent content of A-gellan and F-chitosan/A-gellan hydrogels in PBS and deionized water, respectively.

uptake increases sharply at the beginning then slows down and reaches a steady value after a period of time. Also, the degree of swelling decreased with the increasing content of chitosan fibers in the hydrogels. Actually, there are two opposite factors account for it. The protonation of the free amino groups in chitosan fibers can improve the swelling degrees of F-chitosan/A-gellan hydrogels. The protonation promotes the solubility of the polymeric segments and leads to polymer chain repulsion, so the interactions between amino groups and water molecules allow F-chitosan/A-gellan hydrogels uptake more water into its 3D network (Silva et al., 2008). However, the fibriform chitosan in A-gellan hydrogels would hinder the movement of A-gellan macromolecular segments, thus restrict the changing of A-gellan networks to a great extent, which have already been discussed in the morphology analysis of fractured surface. The macro effects play a leading role in the swelling process, so the F-chitosan/A-gellan hydrogels show lower swelling degrees. Specifically, the swelling degree of the A-gellan hydrogel is more than 1150%, much higher than that of 2.0 F-chitosan/A-gellan hydrogel (750%).

Fig. 3b shows the balancing water content for A-gellan and F-chitosan/A-gellan hydrogels in deionized water and PBS, respectively. Results showed that all the hydrogels immersed in deionized water show higher balancing water content than in PBS. The ionic strength of PBS is much stronger than that of deionized water, which in result reduces the osmotic pressure gap between the hydrogel and the external solutions (Li, Kim, Siddaramaiah, & Lee, 2009). However, the equilibrium solution content of each hydrogels immersed in PBS is also greater than 95%, which may restricts its application to some extent.

3.4. Dehydration kinetic analysis

The DSC curves of A-gellan and 2.0 F-chitosan/A-gellan hydrogels at different heating rates (β_i = 1, 2, 3, 4 and 5 °C min^{-1}) are given in Fig. 4. Both the endothermic enthalpy ΔH_0 and the peak temperature of A-gellan and 2.0 F-chitosan/A-gellan hydrogels increase with increasing heating rate. However, at the some heating rate, the A-gellan hydrogel shows higher endothermic enthalpy than 2.0 F-chitosan/A-gellan hydrogel, this is due to the fact the A-gellan hydrogel has a higher equilibrium swelling ratio than 2.0 F-chitosan/A-gellan hydrogel, which need more quantity of heat to evaporate its water.

The activation energy of the hydrogel is determined by the Kissinger–Akahira–Sunose (KAS) isoconversional method (Akahira & Sunose, 1969; Kissinger, 1957). The KAS method used the Coats-Redfern approximation of the temperature integral, which was considered to be the most practical and accurate method among approximations of temperature integral (Coats & Redfern, 1964). The KAS equation can be described in Eq. (3).

$$\ln\left(\frac{\beta_i}{T_{\alpha,i}^2}\right) = \text{Const} - \left(\frac{E_a}{RT_{\alpha,i}}\right) \quad (3)$$

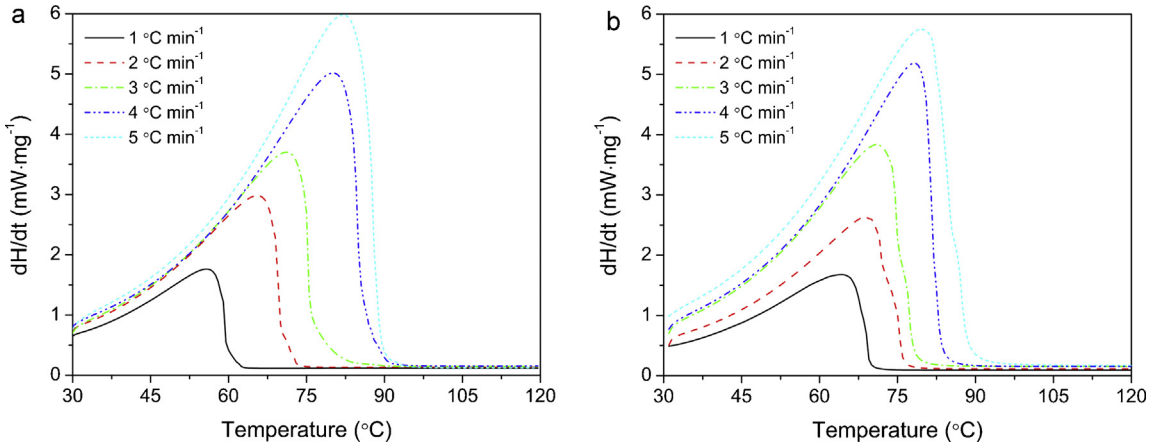

Fig. 4. DSC curves of (a) A-gellan and (b) 2.0 F-chitosan/A-gellan hydrogels.

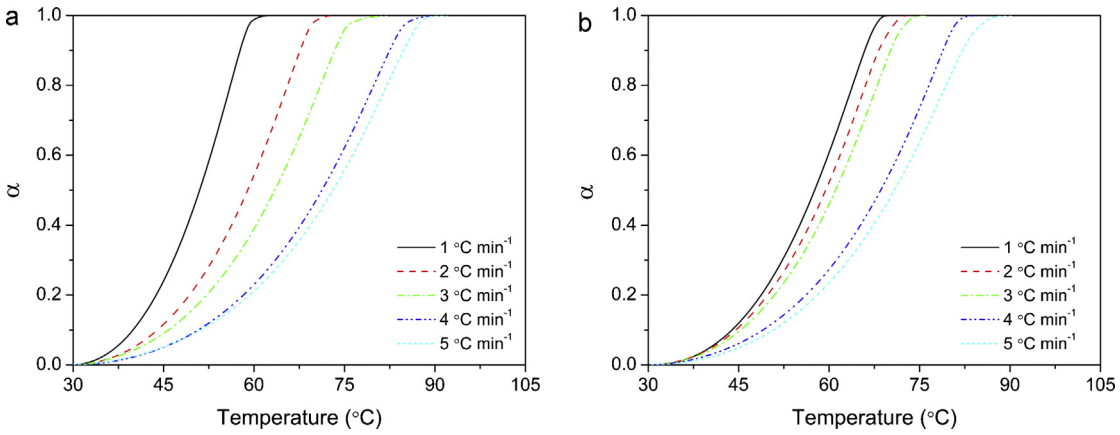

Fig. 5. The relationship between the conversion and temperature for the non-isothermal dehydration of A-gellan and 2.0 F-chitosan/A-gellan hydrogels at different heating rates.

where the subscripts α and i indicate the selected values of the degree of evaporation and heating rate, respectively, E_a is the activation energy, T is the absolute temperature, and R is the universal gas constant.

Fig. 5 shows the dependence of conversion rate (α) on temperature at different heating rates for dehydration process of the A-gellan and 2.0 F-chitosan/A-gellan hydrogels. Then, we plot $\ln(\beta_i/T^2_{\alpha,i})$ vs. $1000/T_{a,i}$, in which β_i and $T_{a,i}$ are obtained from Fig. 5, they should be straight lines with the slope proportional to the activation energy (Fig. 6). Fig. 7a represents the established dependence of E_a on α for the dehydration of A-gellan and 2.0 F-chitosan/A-gellan hydrogels. When α varies from 0.1 to 0.9, the dehydration activation energy of 2.0 F-chitosan/A-gellan hydrogel is decreasing from 210 kJ mol^{-1} to 91 kJ mol^{-1}, which is twice as much as of A-gellan hydrogel at the same α. Though with lower enthalpy of vaporization, the 2.0 F-chitosan/A-gellan hydrogel shows the higher activation energy compared to A-gellan hydrogel. Actually, they are determined by two different factors. The vaporization enthalpy of hydrogel is related to its water content, the hydrogel with high water content means that there is big space in the hydrogel network to accommodate the water, and thus 2.0 F-chitosan/A-gellan hydrogel shows low enthalpy of vaporization because of its low equilibrium water content. However, the dehydration activation energy of hydrogel is determined by the diffusion process of water molecule (Kucerík et al., 2011). The higher activation energy of the 2.0 F-chitosan/A-gellan hydrogel indicates that the macromolecular network-water interaction is more strong and reflecting more excellent water-holding properties.

In non-isothermal kinetics analysis, the choice for a more reasonable mechanism function is very important for us to understand the actual dynamics process. Malek method proposed by Malek and Sestak is a preferable way to confirm the most probable mechanism function for dehydration process (Sestak & Malek, 1993). The application of Malek procedure employs the auxiliary function $Y(\alpha)$, given below:

$$Y(\alpha) = \left(\frac{T}{T_{0.5}}\right)^2 \frac{(d\alpha/dt)}{(d\alpha/dt)_{0.5}} \quad (4)$$

where the $T_{0.5}$ and $(d\alpha/dt)_{0.5}$ are the temperature and reaction rate when $\alpha = 0.5$, respectively.

Here we chose α–T data at a heating rate of 1 °C min^{-1} for the dehydration of the A-gellan and 2.0 F-chitosan/A-gellan hydrogels. Then we take a_i, T_i, $(d\alpha/dt)_i$ (list in Table 1) into the Eq. (4), and obtain the $Y(\alpha)$ vs. α curves which are shown in Fig. 7b. We observed that there are two distinct stages over the whole α. Combine the actual dehydrate process and standard curves given by Malek. We suggested the Zhuralev-Lesokin-Tempelman equation and Mampel power law were suitable for the whole dehydrated process (Noisong & Danvirutai, 2010). In the first stage, the water molecules in the hydrogel's networks abide by the 3D diffusion, however, with the reduction of water, the nucleation dominates the dehydration process of hydrogels, which corresponds to the Mampel power law. Additionally, we can see from Fig. 7b that two curves show similar trend over the whole α, but different values of $Y(\alpha)$ with the same α. Therefore, the chitosan fibers ensure the original

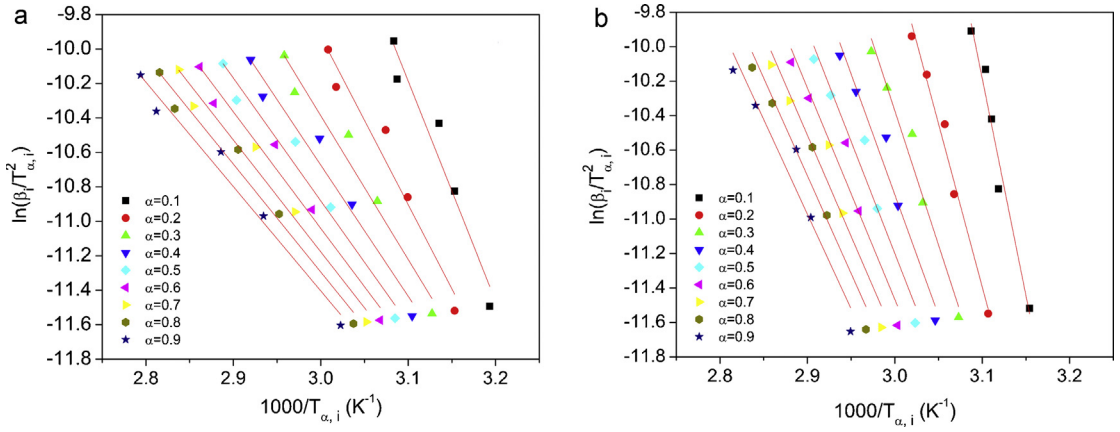

Fig. 6. The relationship curves between $\ln(\beta_i/T^2_{\alpha,i})$ and $1000/T_{a,i}$ using the KAS equation.

Table 1
The dependence of reaction rate on α of A-gellan and 2.0 F-chitosan/A-gellan hydrogels.

α_i	0.1	0.2	0.3	0.4	0.5	0.6	0.7	0.8	0.9
$d\alpha/dt$ (A-gellan)	0.04383	0.05052	0.05487	0.05677	0.05531	0.04847	0.03249	0.01586	0.2116
$d\alpha/dt$ (2.0 F-chitosan/A-gellan)	0.03531	0.0454	0.05055	0.05237	0.04617	0.0377	0.02183	0.00596	0.1529

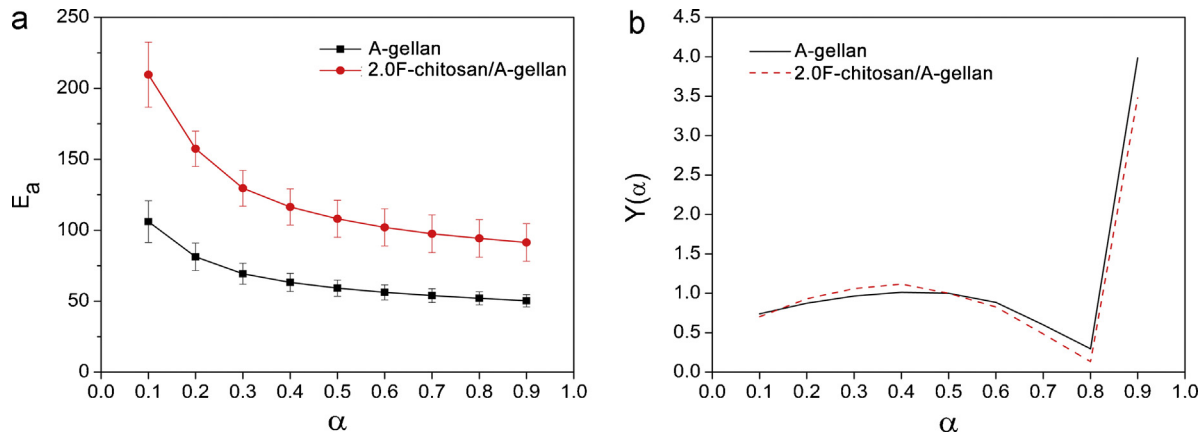

Fig. 7. (a) The dependence of activation energy E_a on α for the dehydration of A-gellan and 2.0 F-chitosan/A-gellan hydrogels. (b) The dependence of $Y(\alpha)$ on α of A-gellan and 2.0 F-chitosan/A-gellan hydrogels.

advantages of A-gellan hydrogel because of the some dehydration process of the A-gellan and 2.0 F-chitosan/A-gellan hydrogels.

3.5. Dielectric properties

As we know, the hydrophilic groups tend to form a strong interaction with water molecules, which play an important role in the water-holding property (Pawde & Deshmukh, 2008); here we make a qualitative comparison of hydrophilism by analyzing the dielectric properties of both the dried A-gellan and 2.0 F-chitosan/A-gellan hydrogels.

The value of the dielectric constant (ε') depends on the polarization behavior of various molecular groups. In terms of dry gel, the orientation polarization of polar groups on the chains is the major contributor to the dielectric constant (Sheinerman, Norel, & Honig, 2000). Fig. 8 shows the dielectric constant and dielectric loss tangent curves at different frequencies of A-gellan hydrogel and 2.0 F-chitosan/A-gellan hydrogel. it shows that the dielectric constant of 2.0 F-chitosan/A-gellan hydrogel at 1 Hz is 878, which is 1.69 times as much as that of A-gellan hydrogel (ε' = 519). This enhancement is attributed to the abundant amino groups in chitosan fibers. The amino group is polar group, as well as hydrophilic group (Kumar, Bristow, Smith, & Payne, 2000). Therefore, there is a close relationship between the dielectric constant and water-holding property of the gels. The significant improvement of dielectric constant indicated the good water-holding property of 2.0 F-chitosan/A-gellan gel, which is identical to the higher activation energy compare to A-gellan hydrogel. In addition, A-gellan and 2.0 F-chitosan/A-gellan gel show different change trends of dielectric loss tangent ($\tan\delta$) over the entire frequency. The $\tan\delta$ of A-gellan dry gel decreases with increasing frequency, but there is a platform on the $\tan\delta$ curve of dried 2.0 F-chitosan/A-gellan gel at the frequency region from 10^2 to 10^3 Hz, which is caused by the slower polarization relaxation time of chitosan fibers.

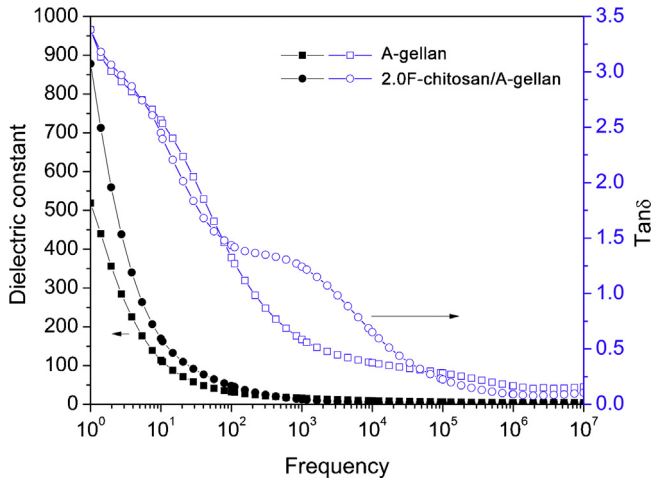

Fig. 8. The curves of dielectric constant and dielectric loss of A-gellan and 2.0 F-chitosan/A-gellan hydrogels.

4. Conclusion

In this paper we developed fiber reinforced F-chitosan/A-gellan hydrogels. The storage moduli increases with the increasing content of chitosan fibers, the storage moduli at 1 rad/s of 2.0 F-chitosan/A-gellan is approximately 4.6 times more than that of the A-gellan hydrogel, which is also confirmed by the fracture morphology analysis. Besides, during the dehydrating process, the chitosan fibers support the macrostructure of 2.0 F-chitosan/A-gellan hydrogels and improve the whole structural stability.

Compared to the A-gellan hydrogel, the addition of chitosan fibers in hydrogels would decrease the equilibrium water content, so the vaporization enthalpy of 2.0 F-chitosan/A-gellan hydrogel is less than the A-gellan hydrogel in the process of dehydration. However, the 2.0 F-chitosan/A-gellan hydrogel shows higher activation energy because of the abundant polar and hydrophilic amino group in chitosan fibers, which also enhanced the dielectric constant and water-holding capacity of 2.0 F-chitosan/A-gellan gel. Given the high performance of F-chitosan/A-gellan hydrogel, the method developed in our work could be offer a useful reference to in the preparation of the scaffold materials.

References

Akahira, T., & Sunose, T. (1969). Trans 1969 joint convention of four electrical institutes.

Brazel, C. S., & Peppas, N. A. (1995). Synthesis and characterization of thermo- and chemomechanically responsive poly(*N*-isopropylacrylamide-co-methacrylic acid) hydrogels. *Macromolecules*, *28*, 8016–8020.

Coats, A. W., & Redfern, J. P. (1964). Kinetic parameters from thermogravimetric data. *Nature*, *201*, 68–69.

Coutinho, D. F., Sant, S., Shakiba, M., Wang, B., Gomes, M. E., Neves, N. M., et al. (2012). Microfabricated photocrosslinkable polyelectrolyte-complex of chitosan and methacrylated gellan gum. *Journal of Materials Chemistry*, *22*, 17262–17271.

Fan, J. B., Gong, Y. H., Ren, L., Varshney, R. R., Cai, D. Z., & Wang, D. A. (2010). In vitro engineered cartilage using synovium-derived mesenchymal stem cells with injectable gellan hydrogels. *Acta Biomaterialia*, *6*, 1178–1185.

Suh, F. J. K., & Matthew, H. W. T. (2000). Application of chitosan-based polysaccharide biomaterials in cartilage tissue engineering: a review. *Biomaterials*, *21*, 2589–2598.

Kissinger, H. E. (1957). Reaction kinetics in differential thermal analysis. *Analytical Chemistry*, *29*, 1702–1706.

Kucerík, J., Prusová, A., Rotaru, A., Flimel, K., Janecek, J., & Conte, P. (2011). DSC study on hyaluronan drying and hydration. *Thermochimica Acta*, *523*, 245–249.

Kumar, G., Bristow, J. F., Smith, P. J., & Payne, G. F. (2000). Enzymatic gelation of the natural polymer chitosan. *Polymer*, *41*, 2157–2168.

Li, P., Kim, N. H., Siddaramaiah, & Lee, J. H. (2009). Swelling behavior of polyacrylamide/laponite clay nanocomposite hydrogels: pH-sensitive property. *Composites Part B: Engineering*, *40*, 275–283.

Liu, C. S., Shao, H. F., Chen, F. E., & Zheng, H. Y. (2006). Rheological properties of concentrated aqueous injectable calcium phosphate cement slurry. *Biomaterials*, *27*(29), 5003–5013.

Muzzarelli, R. A. A. (2009). Chitins and chitosans for the repair of wounded skin, nerve, cartilage and bone. *Carbohydrate Polymers*, *76*, 167–182.

Muzzarelli, R. A. A., Greco, F., Busilacchi, A., Sollazzo, V., & Gigante, A. (2012). Chitosan, hyaluronan and chondroitin sulfate in tissue engineering for cartilage regeneration: A review. *Carbohydrate Polymers*, *89*, 723–739.

Noisong, P., & Danvirutai, C. (2010). Kinetics and mechanism of thermaldehydration of $KMnPO_4 \cdot H_2O$ in a nitrogen atmosphere. *Journal of Industrial and Engineering Chemistry Research*, *49*, 3146–3151.

Oliveira, J. T., Martins, L., Picciochi, R., Malafaya, P. B., Sousa, R. A., Neves, N. M., et al. (2010). Gellan gum: A new biomaterial for cartilage tissue engineering applications. *Journal of Biomedical Materials Research Part A: Applied Biomaterial*, *93A*, 852–863.

Pawde, S. M., & Deshmukh, K. (2008). Characterization of polyvinyl alcohol/gelatin blend hydrogel Films for biomedical applications. *Journal of Applied Polymer Science*, *109*, 3431–3437.

Pelletier, S., Hubert, P., Payan, E., Marchal, P., Choplin, L., & Dellacherie, E. (2001). Amphiphilic derivatives of sodium alginate and hyaluronate for cartilage repair: Rheological properties. *Journal of Biomedical Materials Research*, *54*, 102–108.

Sestak, J., & Malek, J. (1993). Diagnostic limits of phenomenological models of heterogeneous reactions and thermal analysis kinetics. *Solid State Ionics*, *63–65*, 245–254.

Sheinerman, F. B., Norel, R., & Honig, B. (2000). Electrostatic aspects of protein-protein interactions. *Current Opinion in Structural Biology*, *10*, 153–159.

Shin, H., Olsen, B., & Khademhosseini, D. A. (2012). The mechanical properties and cytotoxicity of cell-laden double-network hydrogels based on photocrosslinkable gelatin and gellan gum biomacromolecules. *Biomaterials*, *33*, 3143–3152.

Siegel, R. A., & Firestone, B. A. (1988). PH-dependent equilibrium swelling properties of hydrophobic polyelectrolyte copolymer gels. *Macromolecules*, *21*, 3254–3259.

Silva, S. S., Motta, A., Rodrigues, M. T., Pinheiro, A. F. M., Gomes, M. E., Mano, J. F., et al. (2008). Novel genipin-cross-linked chitosan/silk fibroin sponges for cartilage engineering strategies. *Biomacromolecules*, *9*, 2764–2774.

Smith, A. M., Shelton, R. M., Perrie, Y., & Harris, J. J. (2007). An initial evaluation of gellan gum as a material for tissue engineering applications. *Journal of Biomaterials Applications*, *22*, 241–254.

Swetha, M., Sahithi, K., Moorthi, A., Srinivasan, N., Ramasamy, K., & Selvamurugan, N. (2010). Biocomposites containing natural polymers and hydroxyapatite for bone tissue engineering. *International Journal of Biological Macromolecules*, *47*, 1–4.

Tang, Y. J., Sun, J., Fan, H. S., & Zhang, X. D. (2012). An improved complex gel of modified gellan gum and carboxymethyl chitosan for chondrocytes encapsulation. *Carbohydrate Polymers*, *88*, 46–53.

Tuzlakoglu, K., Alves, C. M., Mano, J. F., & Reis, R. L. (2004). Production and characterization of chitosan fibers and 3-D fiber mesh scaffolds for tissue engineering applications. *Macromolecular Bioscience*, *4*, 811–819.

Vlierberghe, S., Dubruel, P., & Schacht, E. (2011). Biopolymer-based hydrogels as scaffolds for tissue engineering applications: a review. *Biomacromolecules*, *12*, 1387–1408.

Zhu, A. P., Chan-Park, M. B., & Gao, J. X. (2006). Foldable micropatterned hydrogel film made from biocompatible PCL-*b*-PEG-*b*-PCL diacrylate by UV embossing. *Journal of Biomedical Materials Research Part B: Applied Biomaterials*, *76B*, 76–84.